Tale of Two viruses: Two coinfecting archaeal viruses provide insights into virus-virus interactions

Supplementary Material

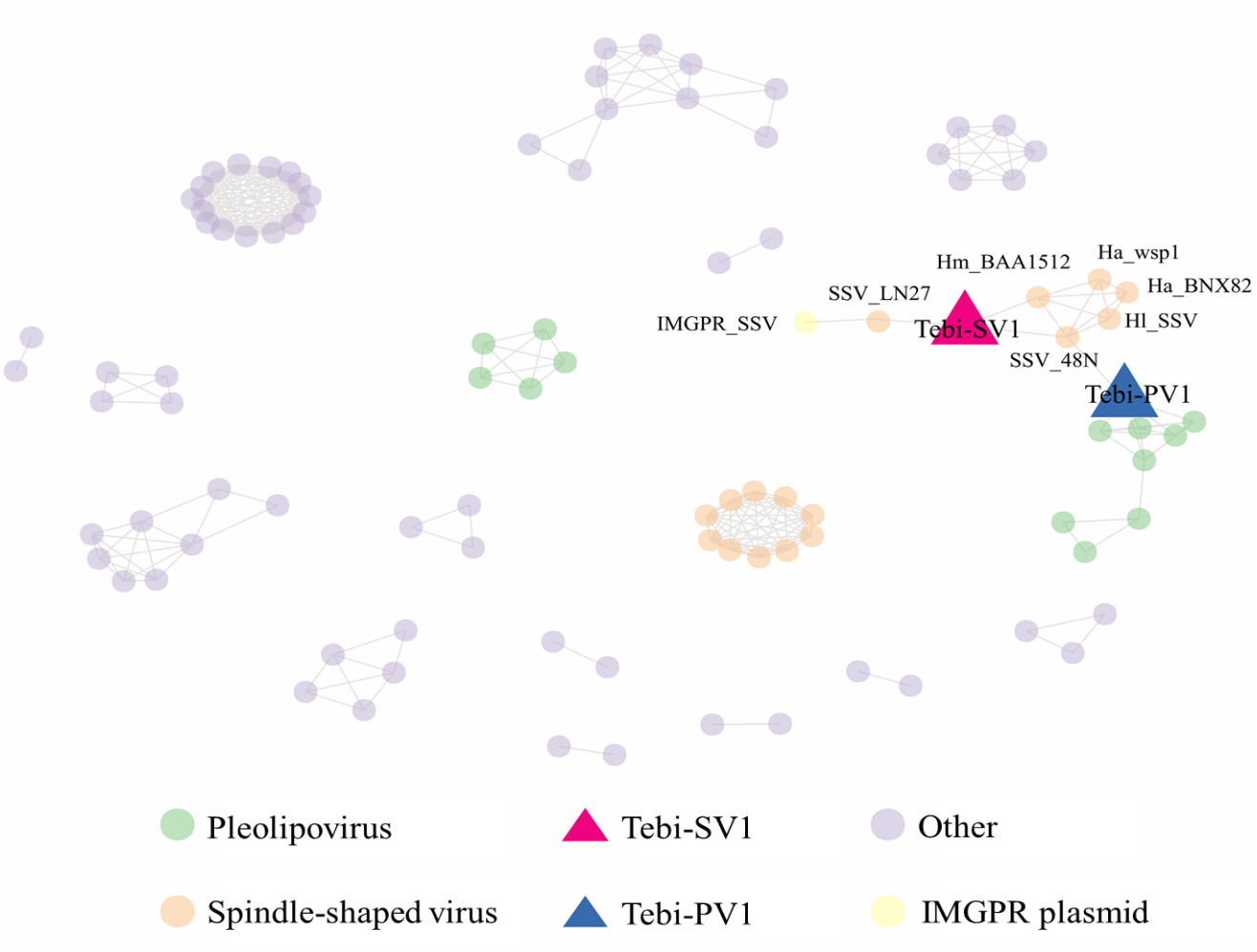

Supplementary Figure 1: Gene sharing network between Tebi-SV1 and Tebi-PV1 and archaeal viruses and plasmids. Circles signify genomes while lines represent shared protein content. Each circle represents a distinct entity Triangles indicate the main viruses of interest (Tebi-SV1 and Tebi-PV1). Tebi-SV1 appears to belong to a distinct group with no similarity to other viruses than those who belong to proposed family, *Almyrocitroviridae*.

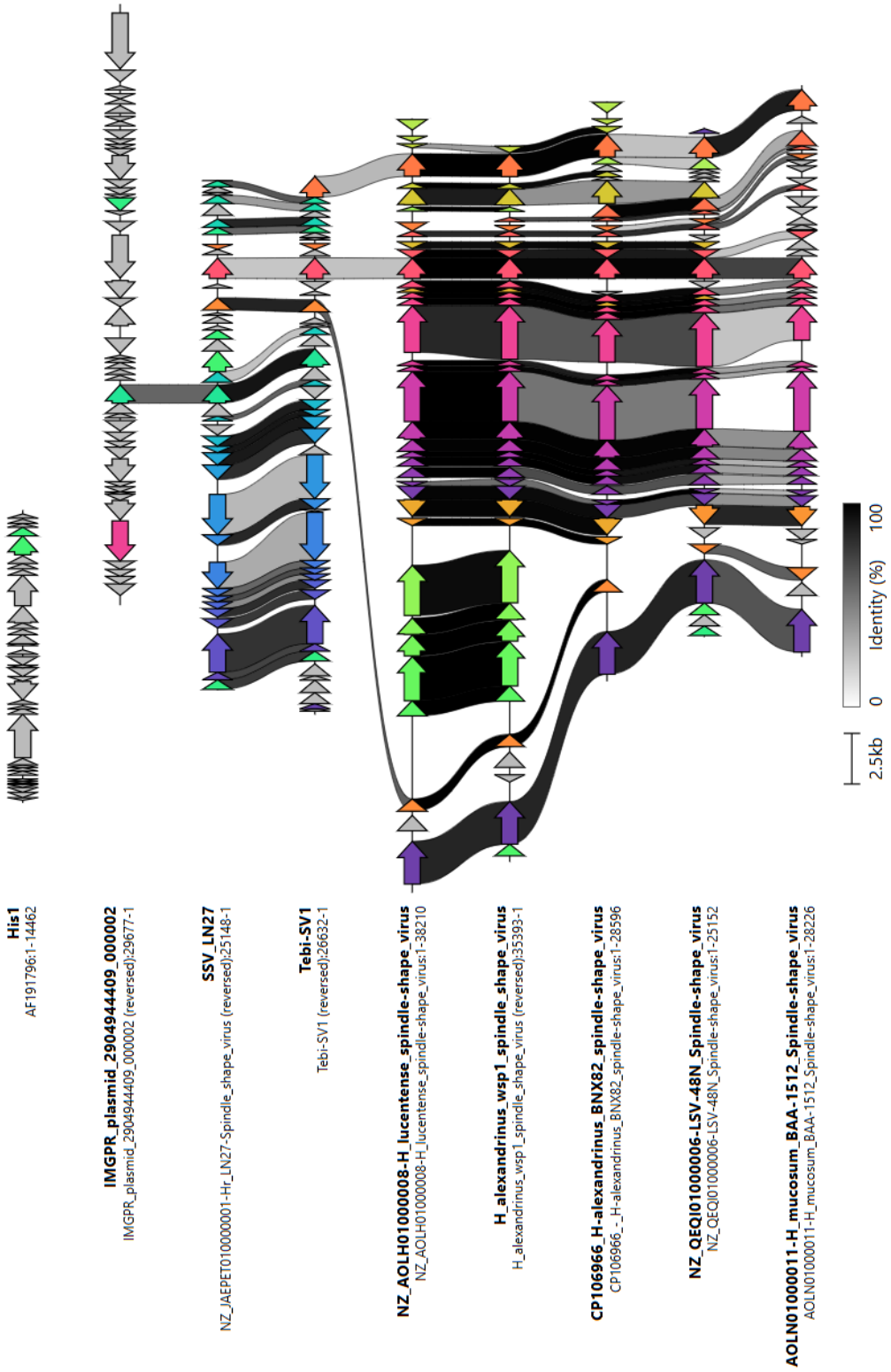

Supplementary Figure 2: Genome comparison of putative spindle-shaped virus genomes of Tebi-SV1-like elements identified from the IMGPR databases as well as previously described spindle-shaped viruses (His1, LSV_48N, and relatives). Homologous genes are shown in the same colors with percent identity represented vertically between genes.

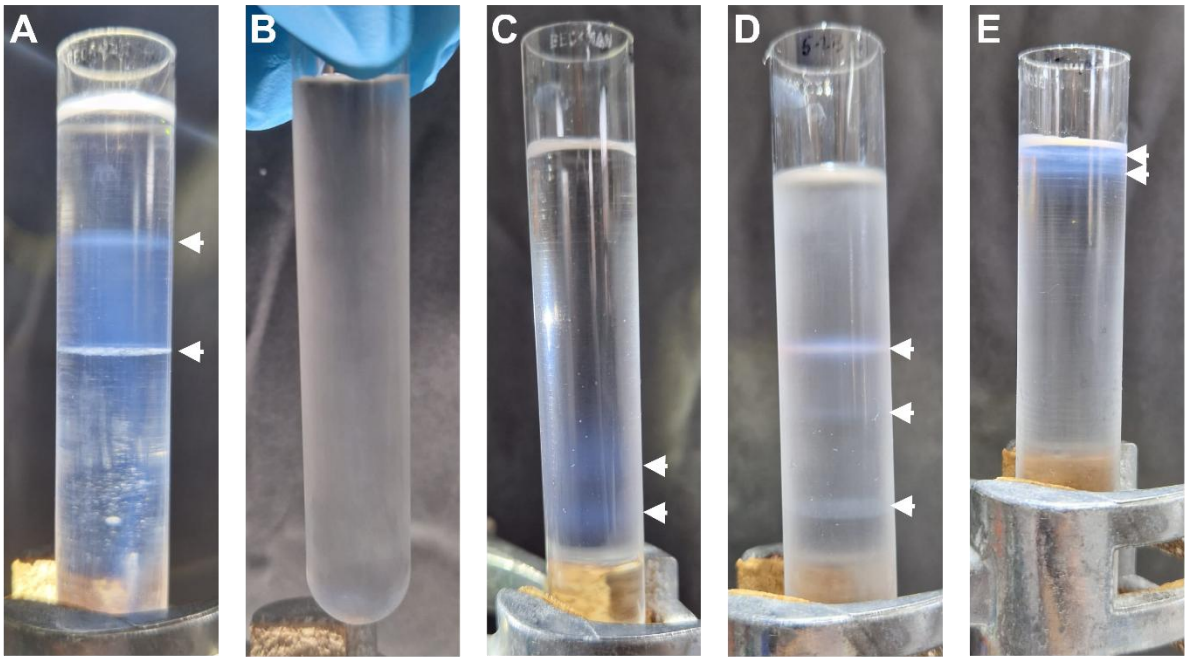

Supplementary Figure 3: Separation of viruses *via* density gradients. All observed bands are indicated with a white arrow. All bands were screened by TEM and PCR for both Tebi-SV1 and Tebi-PV1 (Supplementary Table 3).

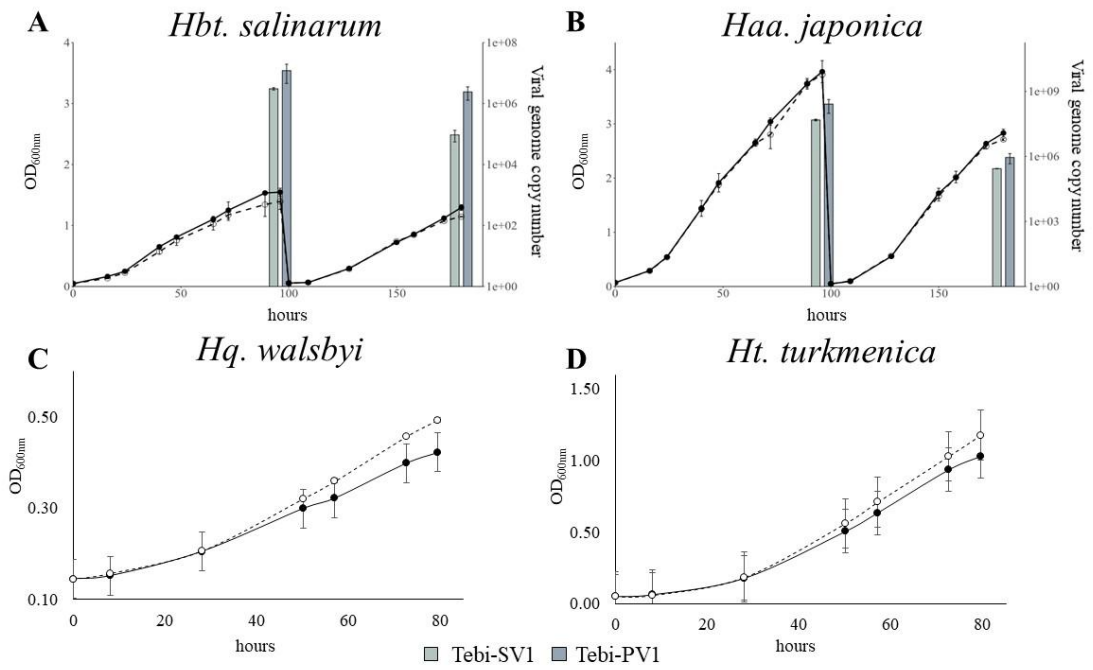

Supplementary Figure 4: Growth curves of infected (broken line) and uninfected (solid line) of four additionally tested host organisms. After reaching stationary phase, cultures (A-B) were diluted to a starting OD600nm of 0.05 and allowed to regrow without additional virus added. Error bars represent the standard deviation of biological triplicates in all curves. Green bars represent the number of Tebi-SV1 genomes per 1.5 mL culture and blue bars represent Tebi-PV1 genomes per 1.5 mL culture detected in the supernatant at 96 and 180 hpi. Error bars represent the standard deviation of n=3 biological replicates (A-B).

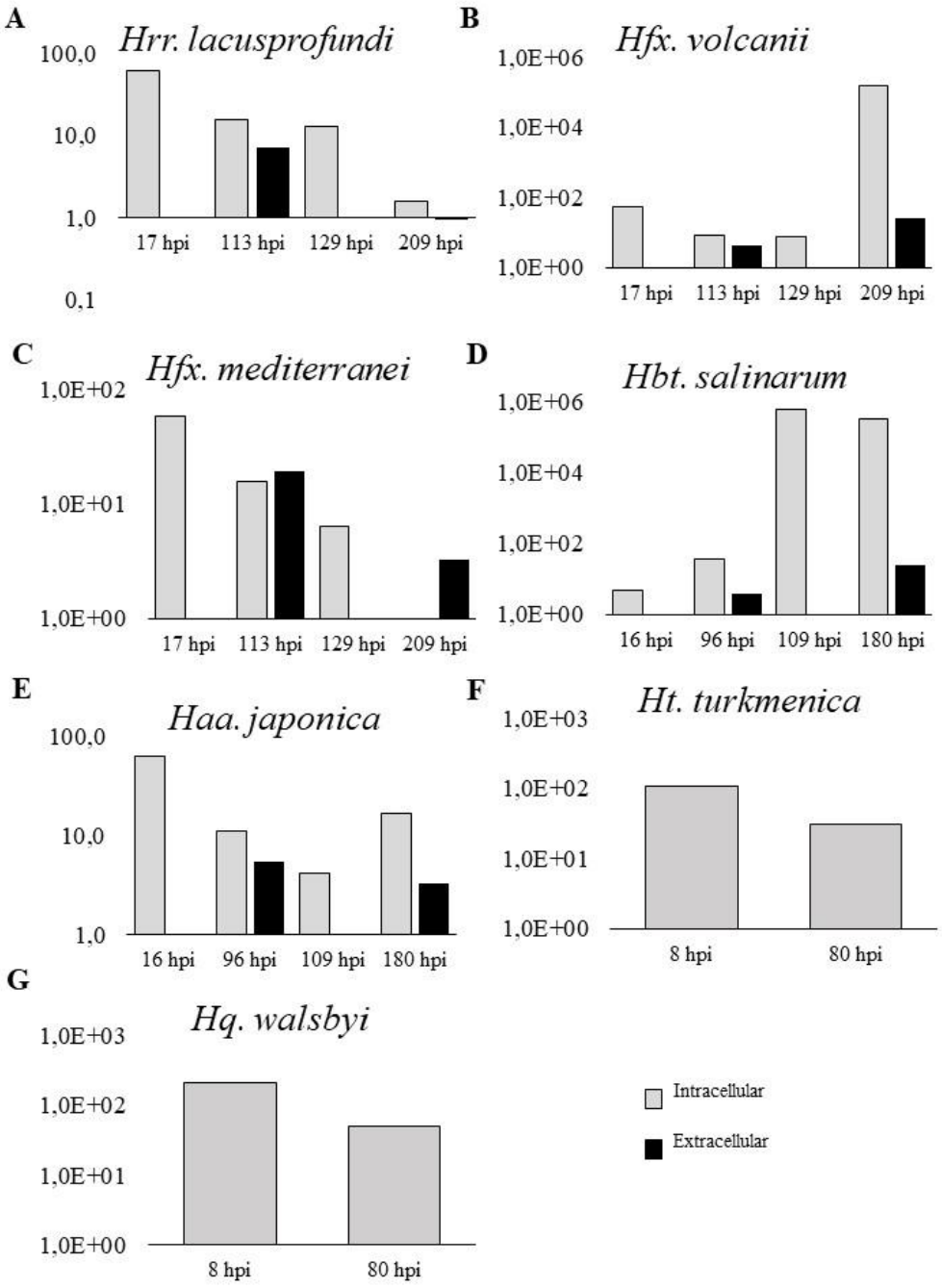

Supplementary Figure 5: Intracellular (grey) and extracellular (black) ratio of genome copy numbers of Tebi-PV1:Tebi-SV1. The number of Tebi-SV1 genomes and Tebi-PV1 genomes were determined by qPCR in cells and the supernatant of 1.5 mL culture (in biological triplicates) and the ratio was determined by dividing the average of Tebi-PV1 numbers with the average of Tebi-SV1 numbers. A value below zero denotes that the number of Tebi-SV1 genomes detected exceeds those of Tebi-PV1. Intracellular Tebi-SV1 numbers became undetectable in *Hfx. volcanii* at 209 hpi (B), therefore, the bar shown only represents Tebi-PV1 numbers.

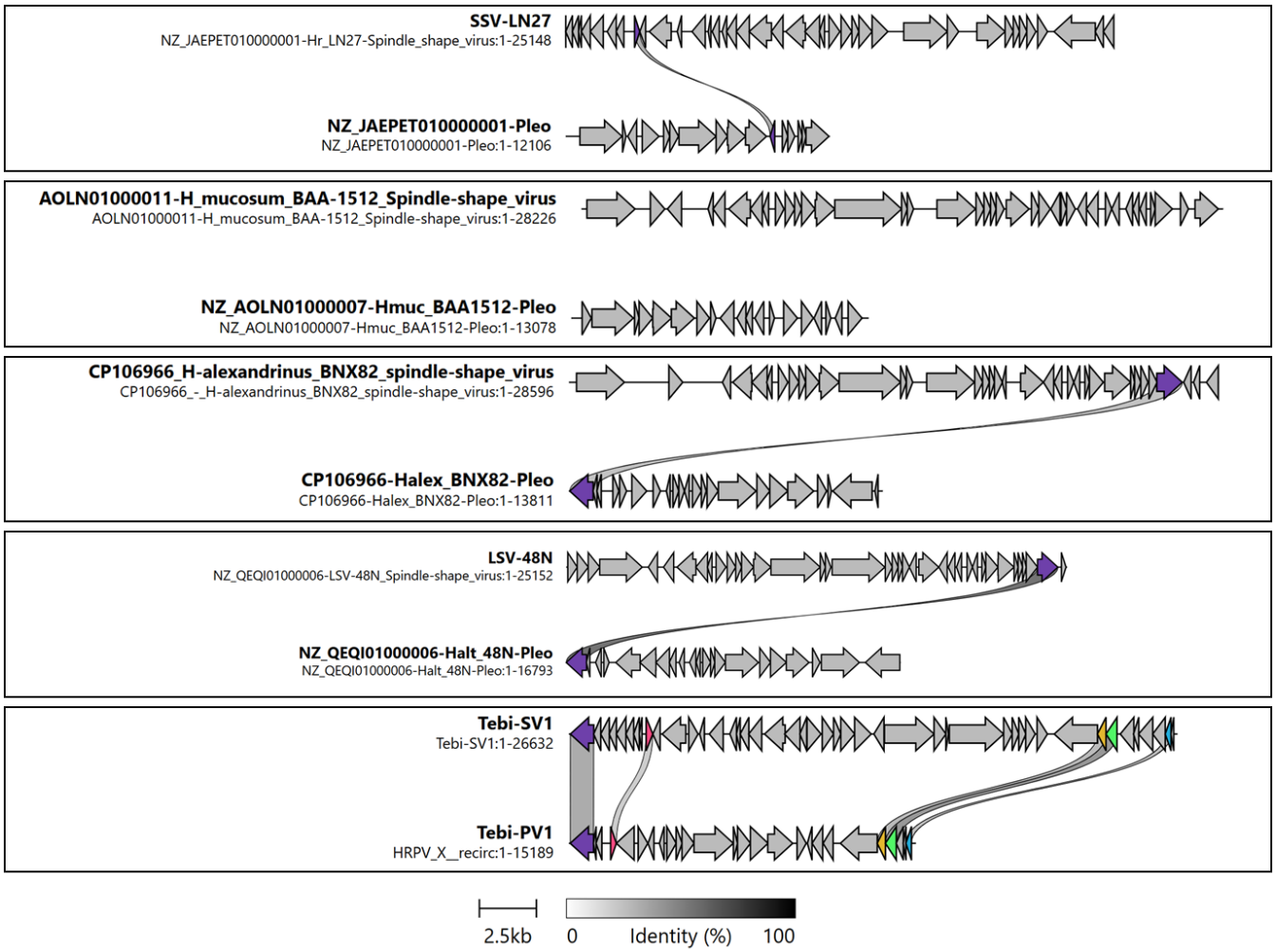

Supplementary Figure 6: Genome comparison of predicted pleolipoviruses within the same host genome of multiple predicted spindle-shaped viruses.

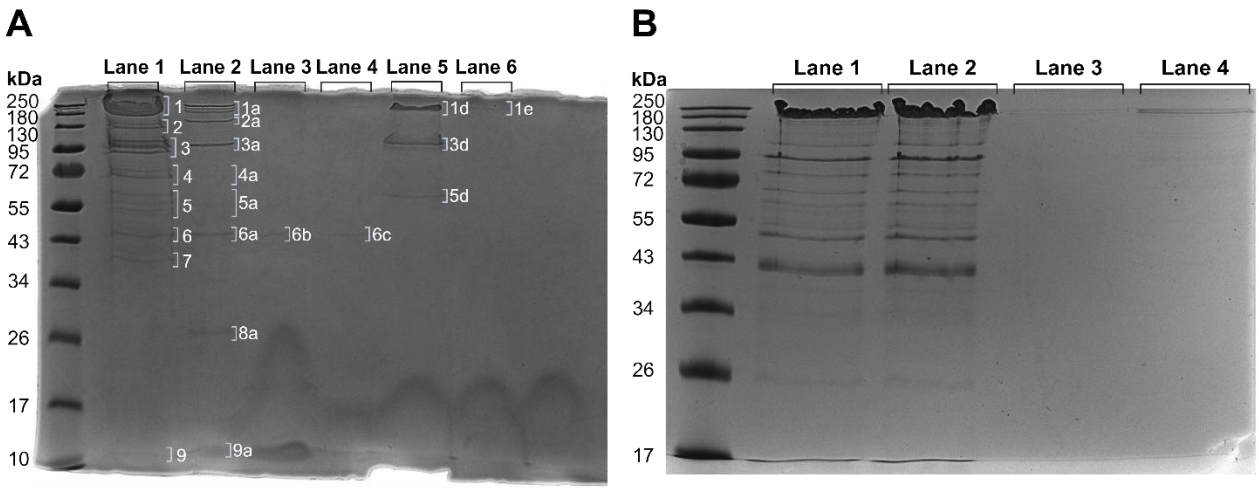

Supplementary Figure 7: Precipitated viral proteins / Virus preparation from *Hrr.* TLS-6 cultures are visualized on 8% acrylamide SDS-PAGE gels. (A) Lane 1 virus preparation from a culture supplemented with 1 mM PO_4 (no gradient purification). Lane 2 is band 2 of a CsCl gradient (Supplementary table 3). Lane 3 and 4 are bands 2 and 3 of an 40-25% Optiprep gradient (Supplementary table 3) from the unpurified sample of Lane 1. Lanes 4-6 are bands 1-3, respectively, of the first virus preparation from *Hrr*. TLS-6, that was sequenced (40-25% Optiprep gradient) (Supplementary table 3). Bands used for MS are labelled with a bracket and the corresponding sample ID found in Supplementary table 5. In (B), Lanes 1 and 2 are biological duplicates of Tebi-PV1 enriched supernatant (no gradient purification) and lanes 3 and 4 are biological duplicates of TLS-6 cellular lysate grown in conditions to enrich for Tebi-SV1.

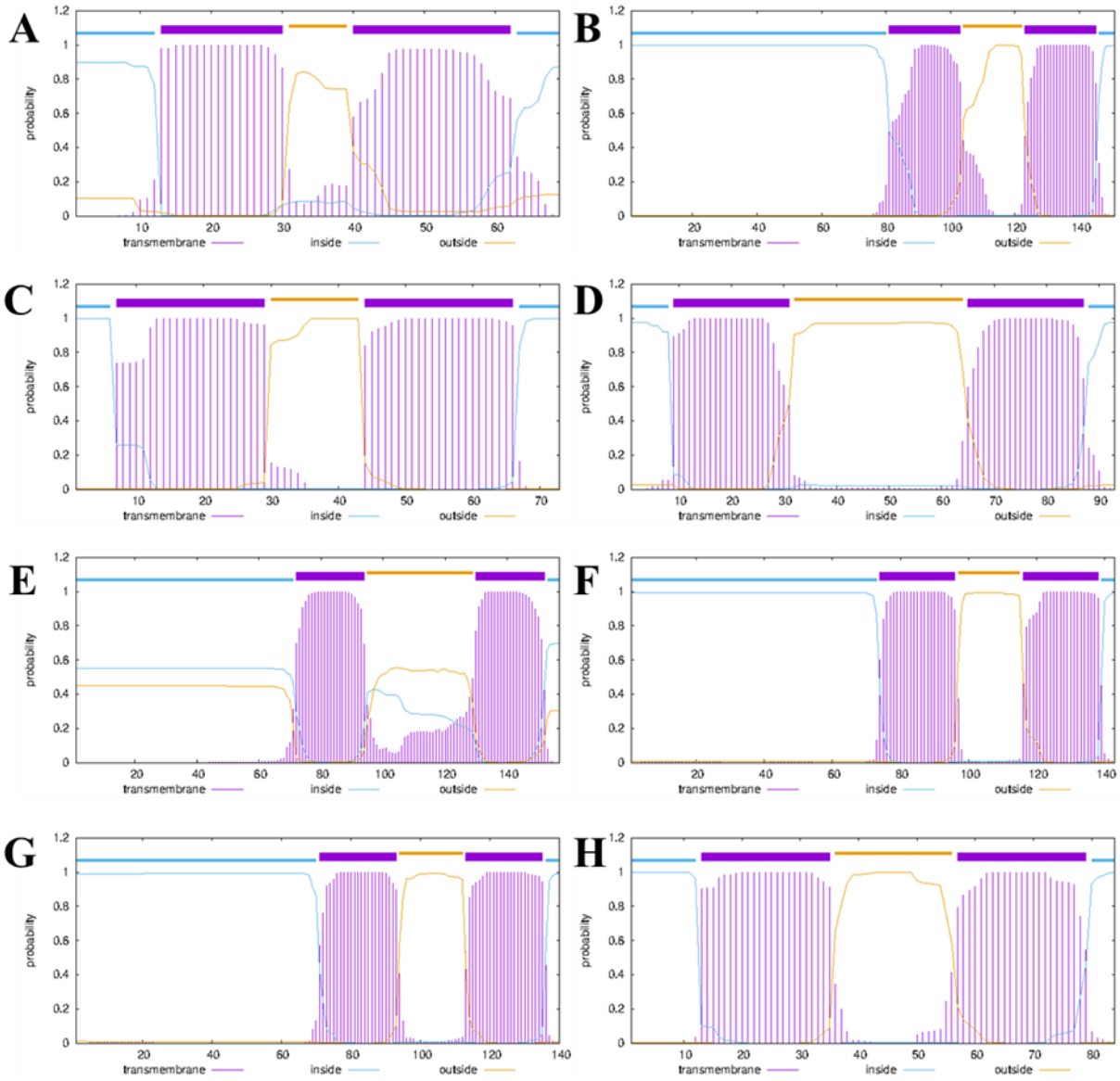

Supplementary Figure 8: TMHMM predictions of transmembrane probabilities using TMHMM server v2.0 for the MCP sequences of spindle-shaped viruses. (A) Tebi-SV1 VP12, (B) Tebi-SV1 VP35, (C) His1 VP21, (D) SSV3 ORF2, (E) SMV1 7RO2_1, (F) SSV5 VP1, (G) ASV1 VP1, and (H) SSV19 7XDI_1

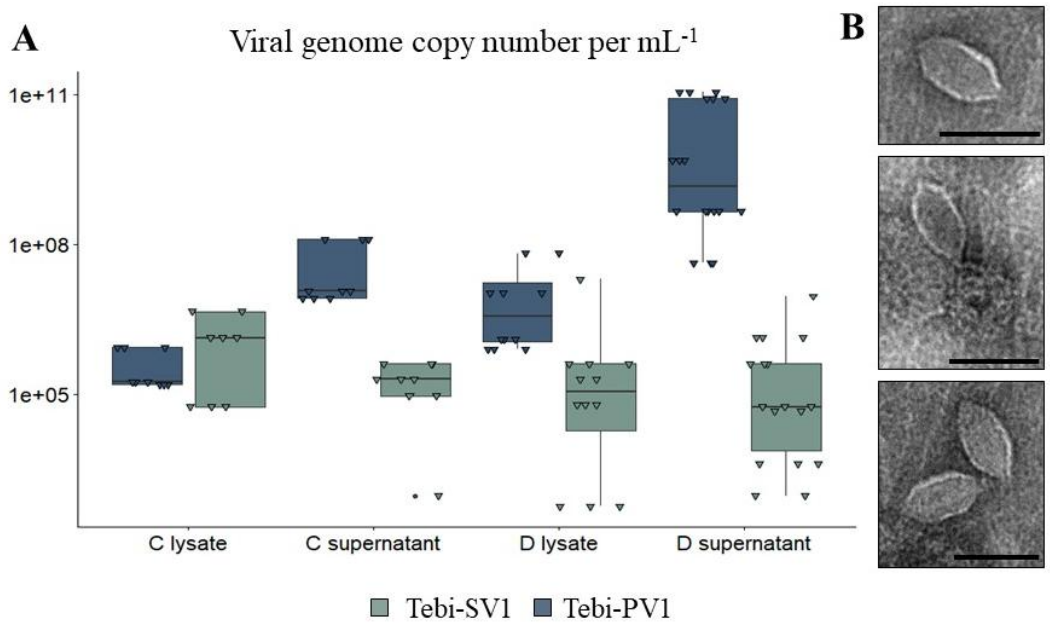

Supplementary Figure 9: Virus particles can be isolated from cell lysates. (A) Box plot of viral genome copy number per mL from lysed cells as well as from the supernatant of *Hrr*. TLS-6. D denotes "nutrient rich" medium, DBCM2+ and C denotes "nutrient deficient" medium, CDM supplemented with 1 mM PO_4. Single dots represent individual biological replicates, vertical line in the box represent the median of n=8 (C lysate and C supernatant) and n=12 biological replicates, whiskers (horizontal lines) show smallest and largest observations. (B) Electron micrographs of Tebi-SV1 viruses in lysate preparations. Scale bars are 100 nm.

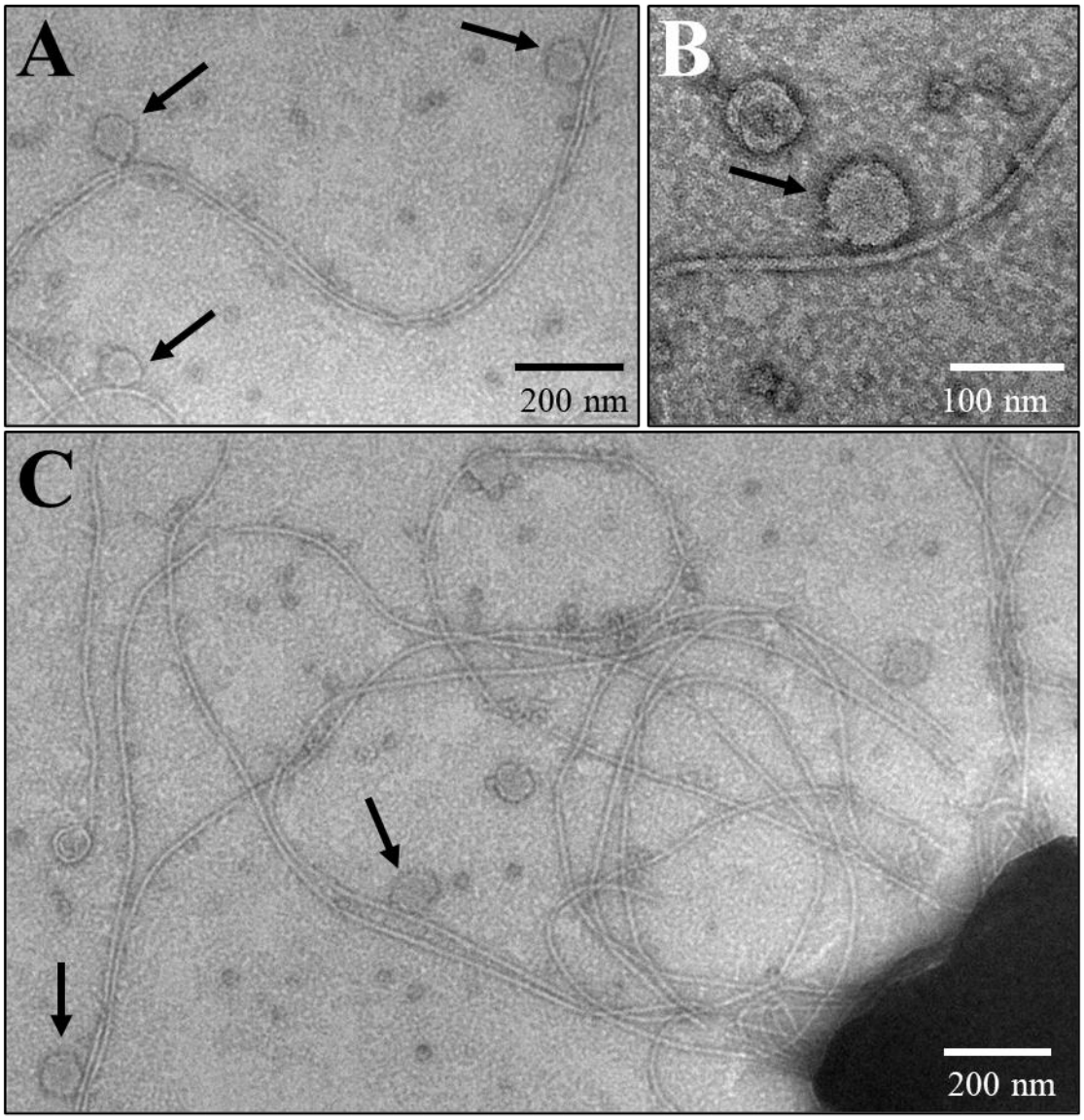

Supplementary Figure 10: Negatively stained micrographs of *Hrr.* TLS-6 cell cultures. (A-C) show Tebi-PV1 virions, denoted by black arrows, attached to cellular appendages.

Supplementary Table 1: Clustering results of Tebi-SV1 and relatives along with other known and unrelated spindle-shaped viruses. The cluster table was reconciled with Victor analysis to indicate the acceptable thresholds of gene-sharing at approximate genus level. The average nucleotide identity (ANI) threshold (95%) used to delineate viral species. The table is included as supplementary data file (.xlsx).

p-value intracellular Tebi-SV1

	DBCM2+ Mitomycin C	DBCM2+ Pravastatin	CDM	CDM + UV	CDM + PO4
DBCM2+	3.28E-01	3.79E-05	7.72E-09		
CDM				4.15E-02	9.07E-03

p-value intracellular Tebi-PV1

	DBCM2+ Mitomycin C	DBCM2+ Pravastatin	CDM	CDM + UV	CDM + PO4
DBCM2+	5.82E-03	2.93E-03	2.69E-03		
CDM				1.42E-06	3.29E-01

p-value extracellular Tebi-SV1

	DBCM2+ Mitomycin C	DBCM2+ Pravastatin	CDM	CDM + UV	CDM + PO4
DBCM2+	4.93E-03	8.75E-01	4.56E-03		
CDM				2.78E-03	9.40E-14

p-value extracellular Tebi-PV1

	DBCM2+ Mitomycin C	DBCM2+ Pravastatin	CDM	CDM + UV	CDM + PO4
DBCM2+	4.57E-01	4.00E-03	3.10E-04		
CDM				9.02E-17	1.35E-09

Supplementary Table 2: Statistical comparison of data presented in Figure 4. Statistical significance is indicated with green for p-value ≤ 0.05 (significant) and red for p-value > 0.05 (not significant).

Supplementary Table 3: Conditions and results from various density gradients as shown in Supplementary figure 2. Each band was observed by electron microscopy. Additionally, each band was DNAse treated and the presence or absence of Tebi-SV1 and Tebi-PV1 genomes was tested by PCR. The table is included as supplementary data file (.xlsx).

Supplementary Table 4: Presence and absence of Pleolipovirus-like proviruses integrated into host genomes where Tebi-SV1 like relatives were identified. Where the absence is indicated by red writing, and genomes with Pleolipoviruses present were described in green text. The table is included as supplementary data file (.xlsx).

Supplementary Table 5: Mass spectrometry data for Tebi-SV1 and Tebi-PV1 particles. Proteome analysis of bands in an SDS-PAGE of virus particles as shown in Supplementary figure 7A. The table is included as supplementary data file (.xlsx).

Supplementary Table 6: All host strains were screened for virus defense systems detected using PADLOC and CRISPRDetect. The table is included as supplementary data file (.xlsx).

Strain ID	Reference	Medium	T (°C)
Halorubrum sp. TLS-6	(Saona et al., 2021)	DBCM2 modified (Mercier et al., 2023) and CDM modified (Nuttall et al., 2008)	28
Halorubrum lacusprofundi ACAM34_UNSW	(Mercier et al., 2023)	DBCM2 modified (Mercier et al., 2023)	28
Halobacterium salinarum 91-R6	(Pfeiffer et al., 2019)	HS media (Pfeiffer et al., 2019)	28
Haloferax mediterranei	(Yang et al., 2015)	HV YPC (Nuttall et al., 2008)	28
Haloferax volcanii DS2	(Hartman et al., 2010)	HV YPC (Nuttall et al., 2008)	28
Haloarcula japonica TR-1	(Horikoshi et al., 1993)	HV YPC (Nuttall et al., 2008)	28
Haloterrigena turkmenica type strain (4kT)	(Saunders et al., 2010)	HV YPC (Nuttall et al., 2008)	28
Haloquadratum walsbyi	(Burns et al., 2007)	Leibniz Institut DSMZ-Deutsche Sammlung von Mikroorganismen und Zellkulturen GmbH ; Curators of the DSMZ; DSM 16854	28

Supplementary Table 7: Host strains used to find virus-free host as well as determine the host range breadth of Tebi-SV1 and Tebi-PV1.

Description	Sequence 5‘ to 3‘	Direction	T (°C)	Type
Tebi-SV1 (qP55-56)	TGTTGTACTACCTCACATC	Forward	59	qPCR
	GAACTACTCACACTAACCA	Reverse		
Tebi-SV1 (qP.Contig 1.3)	CTTCAAAGTGACTGACTC	Forward	60.3	qPCR
	GATAACTGCTGACATCTAC	Reverse		
Tebi-PV1 (qP59-60)	CTACTAACTTCTGGCTAACT	Forward	61	qPCR
	CGAGTCTAGGTAGTTGTAGT	Reverse		
Hrr. lacusprofundi main chromosome	GAGTTAGTGAAGTATCTTCG	Forward	65	qPCR
	GCTCTACATCCTCATAATAC	Reverse		
Hfx. volcanii main chromosome polymerase	CCCGAATCAGGACGAAGAAC	Forward	68	qPCR
	ATTTGAGGTGCTCGGAGAAC	Reverse		
Hfx. mediterranei DNA polymerase	GAAATAAGCGCTGCCTGGAC	Forward	65	qPCR
	GCGTCAAGCACAACATCTC	Reverse		
Tebi-SV1 + restriction site for standard (qP77-78)	GGCCGGAAGCTTTGTTGTACTACCTCACATC	Forward	72	qPCR
	GGCCGGTCTAGAGAACTACTCACACTAACCA	Reverse		
Tebi-PV1 + restriction site for standard (qP81-82)	GGCCGGTCTAGACTACTAACTTCTGGCTAACT	Forward	72	qPCR
	CCGGCCAAGCTTCGAGTCTAGGTAGTTGTAGT	Reverse		
Tebi-SV1 (C)	CTCGGTCTCTCGGATGAAGC	Forward	68	PCR
	GTACTCGTGGATCGTCCGAC	Reverse		
Tebi-PV1 (H)	GCGGCAAACTACCAAGCAAA	Forward	68	PCR
	GGAAATCGCATTGAGACCGC	Reverse		
16S Primer universal (Uni16S)	CCTACGGGNBGCASCAG	Forward	62	PCR
	GACTACNVGGGTATCTAATCC	Reverse		

Supplementary Table 8: All qPCR and PCR primer sequences used in this study with annealing temperature (T °C).